Int J Biochem Mol Biol 2010;1(1):1-11
www.ijbmb.org /ISSN:2152-4114/IJBMB1001001

Original Article

Fluorescence resonance energy transfer (FRET) analysis demonstrates dimer/oligomer formation of the human breast cancer resistance protein (BCRP/ABCG2) in intact cells

Zhanglin Ni*, Michelle E. Mark*, Xiaokun Cai, Qingcheng Mao

Department of Pharmaceutics, School of Pharmacy, University of Washington, Seattle, Washington 98195-7610, USA.

*These two authors contributed equally to this work.

Received January 19, 2010; accepted January 28, 2010; available online February 12, 2010, published August 1, 2010

Abstract: The human breast cancer resistance protein (BCRP/ABCG2) is a half ATP-binding cassette (ABC) efflux transporter that plays an important role in drug resistance and disposition. Although BCRP is believed to function as a homodimer or homooligomer, this has not been demonstrated *in vivo* in intact cells. Therefore, in the present study, we investigated dimer/oligmer formation of BCRP in intact cells. Wild-type BCRP and the mutant C603A were attached to cyan or yellow fluorescence protein and expressed in HEK293 cells by transient transfection. Protein levels, cell surface expression, and efflux activities of wild-type and mutant BCRP were determined by immunoblotting, 5D3 antibody binding, and flow cytometric efflux assay, respectively. Dimer/oligomer formation of BCRP in intact cells was analyzed using fluorescence resonance energy transfer (FRET) microscopy. Wild-type BCRP and C603A were expressed in HEK293 cells at comparable levels. C603A was predominantly expressed in the plasma membrane as was wild-type protein. Furthermore, C603A retained the same mitoxantrone efflux activity and the ability of dimer/oligmer formation as wild-type BCRP. Finally, cross-linking experiments yielded data consistent with the FRET analysis. In conclusion, we have, for the first time, demonstrated that BCRP can form a dimer/oligomer *in vivo* in intact cells using the FRET technique. We have also shown that Cys^{603} alone does not seem to be essential for dimer/oligomer formation of BCRP.

Keywords: BCRP, ABCG2, dimerization, oligomerization, and FRET

Introduction

The human breast cancer resistance protein (BCRP/ABCG2) is the second member of the subfamily G of the large ATP-binding cassette (ABC) transporter superfamily that actively transports a broad spectrum of substrates [1-3]. BCRP expressed on the plasma membrane of cancer cells utilizes the energy provided by ATP hydrolysis to efflux a variety of chemotherapeutic agents out of the cells, thereby conferring multidrug resistance in cancer cells [4]. BCRP is also highly expressed in stem cells [5, 6], in the lumen of the small and large intestines [7], in the liver canalicular membrane [7], in the brain microvessel endothelium [8, 9], and in the apical membrane of placental syncytiotrophoblasts [7, 10]. Due to this pattern of tissue distribution and broad substrate specificity, in addition to its ability of conferring multidrug resistance in cancers, BCRP has been increasingly recognized for its role in drug disposition and protection of tissues from potentially harmful drugs and xenobiotics [1, 11, 12].

Unlike typical ABC transporters such as P-glycoprotein which contain two repeated halves, BCRP consists of only one nucleotide binding domain (NBD) and one membrane spanning domain (MSD) [13, 14]. BCRP also differs from

traditional ABC transporters in that its NBD is at the N-terminus followed by the MSD. This unique domain organization is opposite to that in most of other ABC transporters [12, 15]. Since BCRP is a half ABC transporter, it is widely believed that BCRP functions as a homodimer or a homooligomer possibly formed via intermolecular disulfide bonds [16-18]. The existence of BCRP as a homodimer or a homooligomer has been demonstrated using either purified BCRP or isolated membrane preparations [19, 20]; however, whether BCRP can form a dimer or an oligomer *in vivo* remains to be determined. With respect to specific domains or residues of BCRP that might be critical for dimer/oligomer formation, it has been shown that the region containing residues 528 – 655 appears to be important for oligomerization of BCRP [21]. According to our recently determined topology structure of BCRP [22], this region comprises transmembrane (TM) α-helices 5 and 6, the intracellular loop connecting TM4 and TM5 (residues ~528 – 565), and the extracellular loop connecting TM5 and TM6 (residues ~585 – 622). Whether the entire protein sequence of this particular region is essential for dimer/oligomer formation of BCRP is not known. In addition, three Cys residues in the extracellular loop connecting TM5 and TM6 (Cys^{592}, Cys^{603}, and Cys^{608}) have been intensively studied with respect to their roles in dimer/oligomer formation of BCRP via intermolecular disulfide bonds. These studies showed that Cys^{603} appears to contribute to dimer/oligomer formation of BCRP via an intermolecular disulfide bond, but is not essential for BCRP activity [18, 23, 24]. Since the formation of intermolecular disulfide bonds often accounted for only a fraction of total BCRP protein analyzed in these *in vitro* studies, it has been suggested that artifacts arising from oxidation during sample preparation cannot be excluded [19]. As a result, it has been proposed that some of the intermolecular disulfide bonds identified to be responsible for dimer/oligomer formation of BCRP, including those formed through Cys^{603}, may not actually exist *in vivo* [25]. Such an inconsistency prompted us to further investigate dimer/oligomer formation of BCRP in intact cells and verify some of the previous observations, particularly the role of Cys^{603} in dimer/oligomer formation of BCRP.

Fluorescence resonance energy transfer (FRET) microscopy has emerged as a powerful tool to determine protein-protein interactions *in vivo* in intact cells. FRET microscopy is a quantum physical technique that involves the excitation of an acceptor fluorophore by the emission of a donor fluorophore within a distance range of 10 – 100 Å. This technique has been used to elucidate dimerization/oligomerization of many other membrane proteins in intact cells [26-30], but has not yet been applied to BCRP. In the present study, we used FRET microscopy to elucidate dimer/oligomer formation of BCRP in HEK293 cells, a method that avoids artificial alterations (e.g., formation or breakdown of disulfide bonds) during biochemical sample preparation. To further understand whether Cys^{603} plays an important role in dimer/oligomer formation of BCRP, we generated the mutant C603A and investigated the effect of the mutation of Cys^{603} on dimer/oligomer formation and activity of BCRP.

Materials and methods

Materials

Mitoxantrone (MX) was obtained from Sigma (St. Louis, MO). Fumitremorgin C (FTC) was from the National Cancer Institute (Bethesda, MD). HEK293 cells were purchased from American Type Culture Collection (Manassas, VA). Eagle's minimal essential medium (MEM), phosphate-buffered saline (PBS), 0.25% trypsin-EDTA solution, and Alexa-Fluor488 goat anti-mouse IgG (H + L) were from Invitrogen (Carlsbad, CA). Fetal bovine serum (FBS) was acquired from Hyclone (Waltham, MA). FuGENE HD transfection reagent, the anti-mouse IgG_{2b} (γ2b) peroxidase antibody, and protease inhibitor cocktail tablets were from Roche Applied Science (Indianapolis, IN). All restriction enzymes and T4 DNA ligase were from New England Biolabs (Beverly, MA). The monoclonal mouse anti-BCRP monoclonal antibody (mAb) BXP-21 was from Kamiya Biomedical (Seattle, WA). Primers used for PCR mutagenesis were synthesized by Operon (Huntsville, AL). The pcDNA3.1 plasmid containing full length wild-type BCRP cDNA was a generous gift from Dr. Susan Bates (National Cancer Institute, Bethesda, MD). The pECFP-C1 and pEYFP-C1 plasmids containing cDNAs for cyan and yellow fluorescence protein (CFP and YFP), respectively, were generously provided by Dr. Dan Conrad at the Virginia Commonwealth University. Phycoerythrin-conjugated anti-BCRP mAb 5D3 and the phycoerythrin-conjugated negative control antibody IgG2b were obtained

from eBioscience (San Diego, CA). Fluoromount G was from Southern Biotech (Birmingham, Alabama). Disuccinimidyl suberate (DSS) was purchased from Pierce (Rockford, IL). All other reagents and chemicals were of the highest purity available commercially.

Construction of CFP- or YFP-tagged wild-type BCRP or C603A

The full length BCRP cDNA fragment was amplified using the pcDNA3.1 plasmid containing full length wild-type BCRP cDNA as a template with a forward primer containing a *Xho*I site (5'-CTTCGGCTCGAGCTATGTCTTCCAGTAATGTCGAAG-3') and a reverse primer (5' GTCAGAATCTAGACAAGCTTGGTACCGAGCTCGGATCC-3'). The PCR product was digested with *Xho*I and *Bam*HI (this site is located at the 5'-end of the PCR product) and subcloned into the vector pEYFP-C1 in frame with the YFP coding sequence. The resultant YFP-BCRP plasmid was used as a template for PCR mutagenesis to generate the C603A mutant in which Cys^{603} was replaced with Ala. The primers used to generate C603A were 5'-GCAACAGGAAACAATCCTGCTAACTATGCAACATGTAC-3' and 5'-GTACATGTTGCATAGTTAGCAGGATTGTTTCCTGTTGC-3'. To generate CFP-tagged wild-type BCRP or C603A, the YFP-BCRP plasmids were digested with *Xho*I and *Bam*HI, and the DNA fragments containing wild-type and mutant BCRP cDNAs were subcloned into the pECFP-C1 plasmid. Full length wild-type and mutant BCRP cDNAs as well as the CFP and YFP cDNA sequences in all the constructs were verified by DNA sequencing. In these constructs, CFP or YFP was attached to the N-terminus of wild-type BCRP or C603A. It has been shown that the similar green fluorescence protein attached to the N-terminus of BCRP does not affect its activity [31].

Cell culture and transient transfection

HEK293 cells were grown and maintained in complete culture media (MEM supplemented with 10% FBS, 100 units/ml penicillin, and 100 μg/ml streptomycin). Unless otherwise stated, HEK293 cells were seeded in 65 × 15 mm petri dishes. At approximately 75 – 80% confluence, the cells were transiently transfected with a total of 4 μg of cDNA constructs at a DNA/FuGENE ratio (v/v) of 1:3, according to the manufacturer's instruction. In this 4 μg of cDNA, an equal amount of CFP- and YFP-tagged wild-type BCRP or C603A cDNAs were used at a 1:1 ratio. Twenty four – 48 h after transfection, cells were harvested for whole cell lysate preparation or directly used for flow cytometric assays.

Immunoblotting

Whole cell lysates were prepared from HEK293 cells 24 – 48 h after transfection as previously described [22]. Briefly, cells were harvested with 0.25% trypsin-EDTA, pelleted, and resuspended gently in 150 μl of solubilization buffer (50 mM Tris/HCl, pH 7.5, 10 mM $MgCl_2$, 50 μg/ml phenylmethylsulfonyl fluoride, 0.25% SDS, 250 μg/ml DNase I, and protease inhibitors) and incubated on ice for 1 h. Proteins in the supernatant were collected following centrifugation at 14,000 rpm for 20 min at 4°C and subjected to immunobloting. Whole cell lysates (20 μg of protein each lane) were loaded on a 10% SDS-PAGE mini gel, separated, and transferred onto an Immuno-P nitrocellulose membrane. Protein blots were then blocked with 5% non-fat milk in TBS-Tween buffer (10 mM Tris/HCl, pH 7.5, 0.15 mM NaCl, and 0.05% Tween-20) and probed with the mAb BXP-21 which recognizes an intracellular epitope in the NBD of BCRP [7]. Human β-actin was also detected as an internal control.

Detection of cell surface expression of wild-type BCRP or C603A

The 5D3 antibody recognizes a conformation-sensitive extracellular epitope in BCRP [32]. Binding of the 5D3 antibody to the surface of cells expressing wild-type BCRP or C603A was examined using flow cytometry as previously described [33]. Briefly, 24 – 48 h after transfection, HEK293 cells were harvested with trypsinization and washed once with ice-cold PBS. Cells were resuspended in 0.75 ml of incubation buffer (PBS with 2% BSA) containing 20 μl of either the phycoerythrin-conjugated anti-BCRP mAb 5D3 or the phycoerythrin-conjugated IgG2b negative control for 30 min at 37˚C. Following incubation, cells were immediately placed on ice, washed once with ice-cold PBS, and kept on ice in the dark. Within 1 h, cells were analyzed using a BD FACScan II flow cytometer equipped with a 488-nm argon laser and a 585/42-nm band-pass filter.

Flow cytometric efflux assay

MX efflux activity of wild-type BCRP or C603A was determined using flow cytometry as previ-

ously described [22]. This flow cytometric efflux assay has been widely used to determine BCRP activity for fluorescent substrates [34-36]. Briefly, 24 – 48 h after transfection, HEK293 cells were harvested with trypsinization and washed once with ice-cold PBS. Then, MX efflux activity of cells expressing wild-type BCRP or C603A was determined as previously described [22]. Cells in medium containing MX alone or in medium containing MX and FTC were used to generate the efflux histograms and FTC/efflux histograms, respectively. Since FTC is a potent and specific BCRP inhibitor [37], the difference in median fluorescence (ΔF) between the FTC/efflux and efflux histograms was used as a measure of FTC-inhibitable MX efflux activity of the cells, which is attributable to BCRP or its mutant expression and function.

FRET microscopy and data analysis

HEK293 cells were grown in polystyrene vessels and transiently co-transfected with a total of 1 µg of CFP- and YFP-tagged wild-type BCRP or C603A cDNAs or the CFP/YFP control vectors at a 1:1 ratio as described above. Approximately 24 h after transfection, the cells were washed twice with PBS at room temperature. Subsequently, the cells were fixed with 4% paraformaldehyde for 30 min. Paraformaldehyde was then removed and cells were washed three times with PBS. After that, polystyrene chambers were removed and the cells on glass coverslips were mounted using one drop of 50% glycerol. CFP or YFP images were collected using a Zeiss 510 META confocal microscope equipped with a 63/1.4 oil immersion objective lens. An argon laser (30 mW) was tuned to 458 nm to excite CFP and to 514 nm to excite YFP. An HFT 458/514 dichroic beam splitter was used to deflect the light to the samples. A 470 – 500 nm band-pass filter and a 530 – 600 nm band-pass filter were used in CFP and YFP detection channel, respectively. An NFT 515 beam splitter was used to separate the CFP and YFP emission. FRET was determined with acceptor photobleaching as previously described [38]. In the acceptor photobleaching protocol, cells were scanned in the YFP channels in a defined region of interest (ROI) for 25 iterations using a 514-nm argon laser line at 100% intensity with a pinhole diameter set to 1.00 airy unit to selectively induce acceptor photobleaching. ROIs were corrected for background fluorescence prior to the calculation of FRET efficiencies. FRET efficiency ($FRET_e$) was then estimated using the following equation: $FRET_e = (I_{post} - I_{before})/I_{post} \times 100$, where I_{before} and I_{post} are the donor fluorescence intensity before and after photobleaching of the acceptor, respectively. The experiments were repeated with at least three independent transfections with the acceptor bleached to 25 – 35% of its initial value for each protein pair. The levels of the donor fluorescence intensity in the ROIs, measured as pixel values, were at least 3 times greater than the background. To eliminate a possible crowding effect of protein overexpression, FRET microscopy was performed in defined regions of the plasma membrane with comparable protein expression (as judged by fluorescence intensity) for all the protein pairs and CFP alone.

Chemical cross-linking

To further verify the results of the FRET analysis, chemical cross-linking was performed on intact cells as previously described [39]. Briefly, 24 – 48 h after transfection, cells were incubated at room temperature for 30 min in PBS containing DSS at a final concentration of 2 mM. The reaction was terminated by adding Tris-HCl (pH 8.0) to a final concentration of 20 mM. Cells were then harvested, followed by whole cell lysate preparation and immunoblotting with the BXP-21 antibody as described.

Statistical analysis

Data obtained were analyzed for statistical significance using the Student's *t*-test, and differences with p values of < 0.05 were considered statistically significant.

Results

Expression of wild-type BCRP and C603A in HEK293 cells

An equal amount of CFP- and YFP-tagged wild-type BCRP or C603A cDNAs or the CFP/YFP control vectors were co-transfected into HEK293 cells, and the expression levels of wild-type and mutant BCRP were examined by immunobloting of whole cell lysates. The expression levels of wild-type BCRP and C603A were comparable (**Figure 1A**), indicating that the expression and/or stability of BCRP was not affected by the mutation of Cys^{603}. As expected, no BCRP expression could be detected in cells transfected with the CFP/YFP control vectors only.

Cell surface expression of wild-type BCRP and C603A

We next determined cell surface expression of wild-type BCRP and C603A by measuring binding of the phycoerythrin-conjugated 5D3 to the surface of cells expressing these proteins. As expected, no difference in phycoerythrin fluorescence between the cells treated with 5D3 and the IgG2b control was observed with cells expressing CFY/YFP only (**Figure 1B**). However, cells expressing wild-type BCRP or C603A

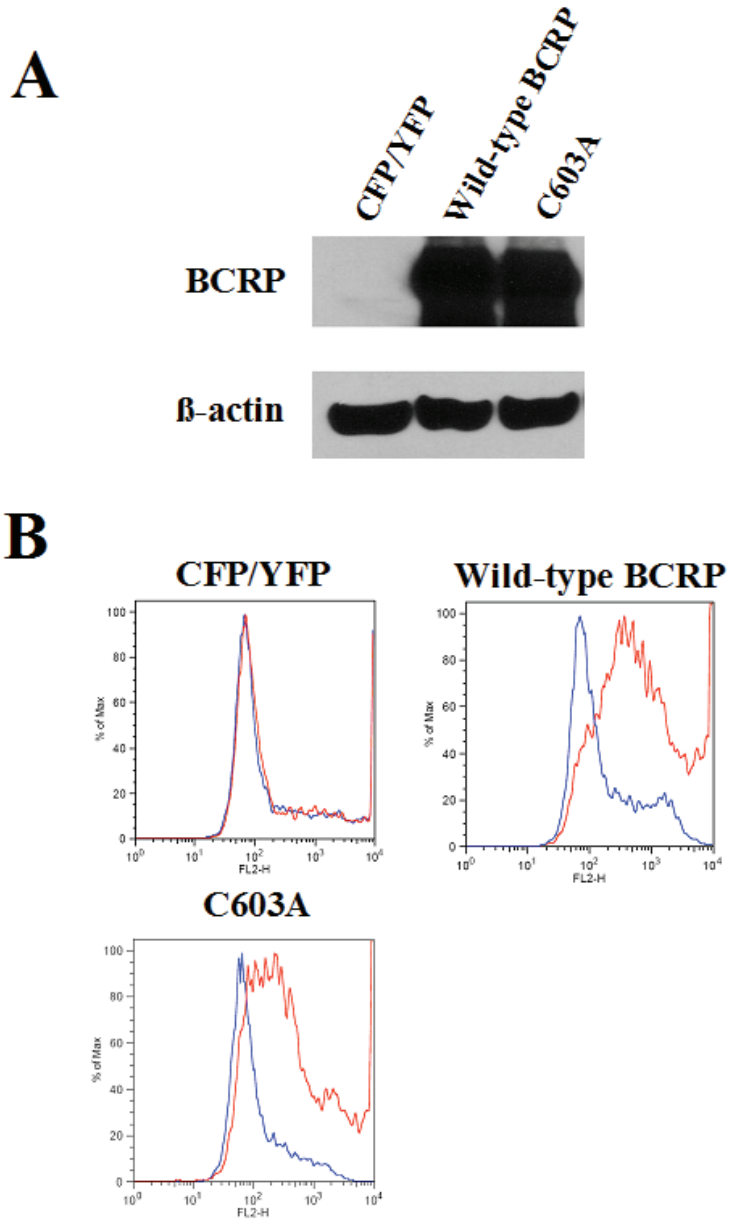

Figure 1. Immunoblot of HEK293 cells co-transfected with CFP/YFP-tagged wild-type BCRP or C603A cDNAs (A) and cell surface expression of wild-type BCRP or C603A (B). A, whole cell lysates (20 µg of protein each lane) prepared from HEK293 cells transiently transfected with CFP/YFP-tagged wild-type BCRP or C603A cDNA constructs or the CFP/YFP control vectors were immunoblotted as described. BCRP was detected with the mAb BXP-21 (upper panel). β-actin expression was also examined as an internal control (lower panel). The constructs (CFP/YFP, wild-type BCRP, and C603A) are indicated above the blots. B, HEK293 cells expressing wild-type BCRP or C603A were processed for determining the 5D3 binding using flow cytometry as described. Phycoerythrin fluorescence associated with the IgG2b control and 5D3 is represented by the blue and red lines, respectively. The histograms for CFP/YFP, wild-type BCRP, and C603A are indicated above the graphs.

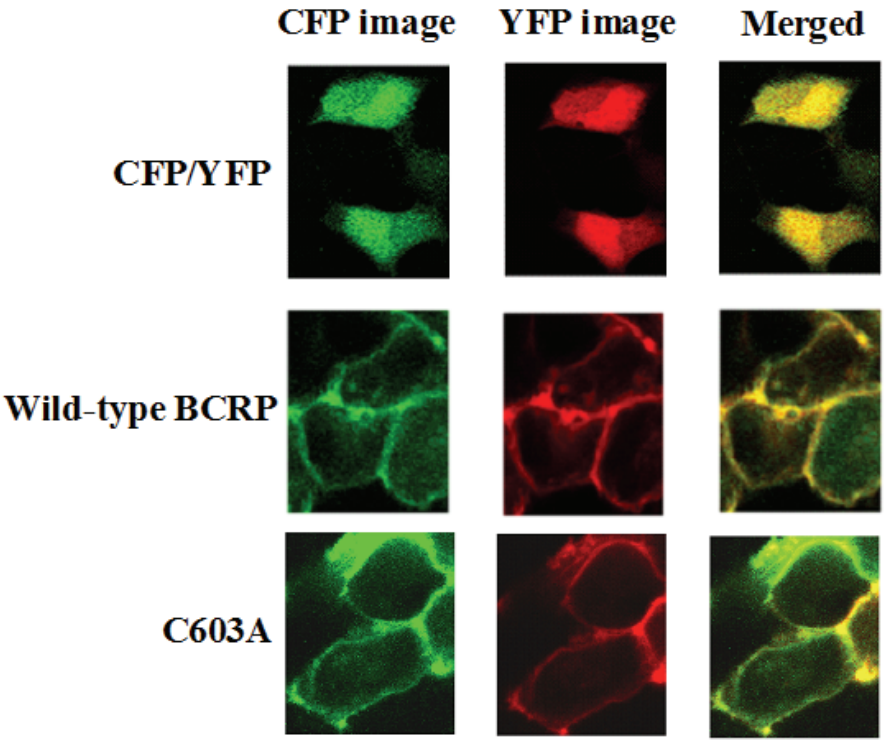

Figure 2. Confocal fluorescence images of HEK293 cells co-transfected with CFP/YFP-tagged wild-type BCRP or C603A cDNAs. HEK293 cells were co-transfected with CFP/YFP-tagged wild-type BCRP or C603A cDNA constructs or the CFP/YFP control vectors and processed for confocal fluorescence microscope analysis as described. Shown are CFP (left), YFP (middle), and merged (right) images. Images for CFP/YFP, wild-type BCRP, and C603A are indicated on the left.

demonstrated a significant shift in phycoerythrin fluorescence between the 5D3 and IgG2b treatments (**Figure 1B**), supporting cell surface expression of wild-type BCRP or C603A, respectively.

Cellular localization of wild-type BCRP or C603A

To determine whether the mutation of Cys^{603} could affect the plasma membrane localization of BCRP, transfected cells were analyzed using confocal fluorescence microscopy. As shown in **Figure 2**, when cells were transfected with the CFP/YFP control vectors only, CFP and YFP were expressed ubiquitously in the cells with no specific targeting to the plasma membrane. The CFP or YFP tag itself was not expected to perturb the topological assembly of BCRP in the plasma membrane because it was attached to the N-terminus of BCRP which is located intracellularly. Thus, in the case of wild-type BCRP or C603A, a strong CFP or YFP fluorescence signal or the signal in the merged image was observed primarily on the plasma membrane (**Figure 2**), suggesting that wild-type BCRP or C603A was predominantly targeted to the plasma membrane of HEK293 cells.

MX efflux activity of wild-type BCRP or C603A

We next determined if the mutation of Cys^{603} affects BCRP efflux activity using a model fluorescent substrate MX. Incubation of cells expressing wild-type BCRP or C603A with the BCRP-specific inhibitor FTC resulted in a similarly significant increase in the intracellular MX accumulation compared to that without FTC treatment (data not shown), suggesting that MX is actively effluxed by wild-type BCRP or C603A. Thus, the FTC-inhibitable MX efflux activities of wild-type BCRP and C603A were comparable (**Figure 3**). The FTC-inhibitable MX efflux activities of cells expressing only the CFP/YFP pair control were significantly lower than those of

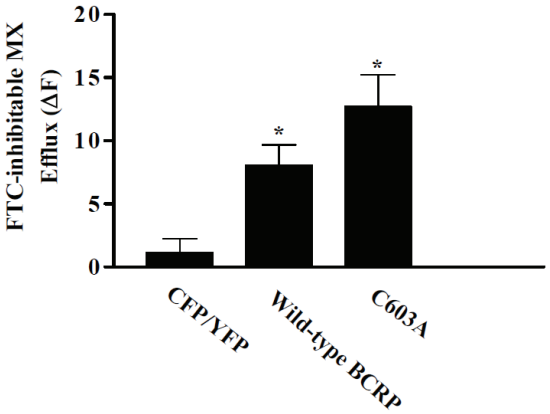

Figure 3. FTC-inhibitable MX efflux activities of wild-type BCRP and C603A. HEK293 cells were co-transfected with CFP/YFP-tagged wild-type BCRP or C603A cDNA constructs or the CFP/YFP control vectors and processed for flow cytometric efflux assay as described. The difference (ΔF) in median MX fluorescence of cells treated with and without FTC was used as a measure of FTC-inhibitable MX efflux activities. Shown are means ± S.D. of at least three independent experiments. Significant difference: * $p < 0.05$ as compared with the efflux activity of CFP/YFP by the Student's *t*-test.

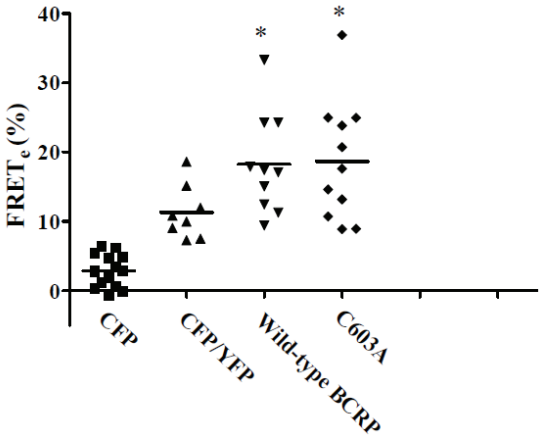

Figure 4. FRET efficiencies of cells co-transfected with CFP/YFP-tagged wild-type BCRP or C603A cDNAs. HEK293 cells were co-transfected with CFP/YFP-tagged wild-type BCRP or C603A cDNA constructs or the CFP/YFP control vectors or the CFP vector alone and processed for determining FRET efficiencies as described. Significant difference: * $p < 0.05$ as compared with the FRET efficiency of the CFP/YFP control by the Student's *t*-test. Horizontal lines show the mean values of FRET efficiencies of each protein pair.

the cells expressing wild-type BCRP or C603A (**Figure 3**). These results suggest that C603A fully retains MX efflux activity comparable to wild-type protein.

Detection of dimer/oligomer formation of wild-type BCRP or C603A by FRET analysis

We then determined the effect of the mutation of Cys^{603} on dimer/oligmer formation of BCRP in intact cells using FRET microscopy. FRET analysis was performed for cells expressing the CFP/YFP pair control, the CFP/YFP-tagged wild-type BCRP or C603A, or CFP alone. The CFP/YFP fluorophore pair was selected for their excellent spectral overlap to allow for efficient energy transfer from the donor (CFP) to the acceptor (YFP). The transfer of energy was measured as an increase in the donor fluorophore emission after photobleaching of the acceptor. FRET efficiencies were then estimated as described. As shown in **Figure 4**, the negative control cells expressing CFP alone showed some increase in donor fluorescence after acceptor photobleaching. FRET efficiencies of the cells expressing the CFP/YFP pair control were increased compared with those of cells expressing CFP alone, suggesting that there was some background caused by overexpression of CFP and YFP due to cross-talk between the two fluorescence proteins (**Figure 2**). However, the FRET efficiencies of cells expressing CFP/YFP-tagged wild-type BCRP were significantly greater than those of cells expressing the CFY/YFP pair control, indicating that the molecules of wild-type BCRP likely interact with each other through the formation of homodimers or homooligomers. The FRET efficiencies of cells expressing CFP/YFP-tagged C603A were comparable to those of cells expressing CFP/YFP-tagged wild-type BCRP, suggesting that C603A retained the same ability to form a dimer/oligomer as wild-type protein.

Chemical cross-linking

To further confirm if the monomers of wild-type BCRP or C603A exist in close proximity in intact cells, we performed chemical cross-linking experiments using the homobifunctional amine-reactive cross-linker DSS (11.4 Å arm length) on intact cells expressing these proteins. Either wild-type BCRP or C603A could be cross-linked as indicated by the appearance of higher mole-

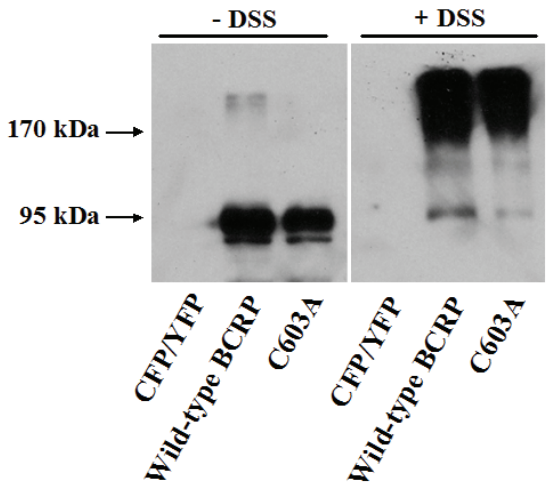

Figure 5. Chemical cross-linking. Chemical cross-linking of wild-type BCRP or C603A on intact cells using DSS was described in the Materials and Methods section. Whole cell lysates prepared from HEK293 cells transiently transfected with CFP/YFP-tagged wild-type BCRP or C603A cDNA constructs or the CFP/YFP control vectors were immunoblotted using the mAb BXP-21 as described. The constructs (CFP/YFP, wild-type BCRP, and C603A) are indicated below the blot. As indicated with arrows, the molecular weight of CFP/YFP-tagged wild-type BCRP or C603A monomer is approximately 95 kDa.

cule mass bands corresponding to dimers and oligomers of the 95 kDa CFP/YFP-tagged BCRP or C603A (**Figure 5**). These data seem to be consistent with the results of the FRET analysis.

Discussion

In the present study, we investigated protein-protein interactions of BCRP molecules in intact cells using the FRET confocal microscopy. This approach allows us to elucidate dimer/oligomer formation of BCRP in a native cellular membrane environment without the need of biochemical sample preparation. To perform the FRET assay, the fluorescent protein CFP or YFP was attached to the N-terminal end of wild-type BCRP or the mutant C603A. The CFP/YFP-tagged fusion proteins of wild-type BCRP were properly expressed and routed to the plasma membrane (Figs. 1 and 2). This suggests that the attachment of CFP or YFP at the N-terminus does not affect proper folding and assembling of BCRP, allowing visualization of plasma membrane targeting and analysis of function and dimer/oligomer formation of BCRP in intact cells. This is consistent with the results of the previous study which demonstrates that BCRP with green fluorescence protein attached at its N-terminus is fully functional [31].

We used acceptor photobleaching FRET assay [38], based on the fact that bleaching of an acceptor fluorophore (YFP) results in an increase in donor fluorescence (CFP), as the transfer of energy from the donor to the acceptor is interrupted. Acceptor photobleaching FRET assay is the easiest and most accurate way to quantify FRET compared to other commonly used FRET assays [40]. To reduce false-positive measurements due to cross-talk in CFP-to-YFP FRET, we deliberately included two negative controls, namely the measurements of CFP alone and CFP/YFP co-transfected. With this method, we estimated the FRET efficiencies of intact cells expressing CFP/YFP-tagged wild-type BCRP or C603A, the CFP/YFP pair control or CFP alone. The FRET efficiencies of CFP/YFP-tagged wild-type BCRP were significantly higher than those of the CFP/YFP pair control (**Figure 4**), suggesting that wild-type BCRP likely forms homodimers or homooligomers *in vivo* in intact cells. Thus, we have confirmed that homodimerization or homooligomerization of wild-type BCRP observed *in vitro* also occurs *in vivo* in intact cells. Moreover, the CFP/YFP-tagged wild-type BCRP was active in transporting MX (**Figure 3**), thus supporting the conclusion that BCRP functions as a homodimer or a homooligomer *in vivo*. Furthermore, the FRET results were consistent with the data obtained from the standard chemical cross-linking experiments (**Figure 5**). It was, however, not possible to distinguish between BCRP dimers and higher order oligomers by the FRET analysis.

Ala substitution of Cys^{603} did not deteriorate expression, plasma membrane localization, and activity of BCRP in HEK293 cells (Figs. 1 – 3), which is in good agreement with previous studies [18, 24, 25]. It has been proposed that Cys^{603} plays an important role for dimer/oligomer formation of BCRP via an intermolecular disulfide bridge. This conclusion was obtained by the demonstration that wild-type BCRP migrated as a band of approximately double the size of a BCRP monomer under non-reducing conditions; however, after Cys^{603} was mutated to Ala, the C603A mutant migrated as a single monomeric band [18, 23, 24]. Nevertheless, at least one study [23] showed that a

substantial amount of C603A and other mutants at position Cys^{603} remained as dimers under non-reducing conditions. It is worth noting that the observation of dimer/oligomer formation of BCRP via intermolecular disulfide bonds has so far been reported all using *in vitro* biochemical methods such as immunoblotting under non-reducing conditions. It is possible that oxidation during biochemical sample preparation may cause formation of intermolecular disulfide bridges or disulfide bonds may be disrupted in the process of cell lysis or sample preparation involving solubilization of membrane proteins with detergents. The FRET assay determines protein-protein interactions in intact cells without biochemical sample preparation. We found that the FRET efficiency of CFP/YFP-tagged C603A was the same as that of CFP/YFP -tagged wild-type BCRP (**Figure 4**), suggesting that Ala substitution of Cys^{603} does not affect the ability of BCRP to form a dimer/oligomer. Chemical cross-linking experiments also indicate that CFP/YFP-tagged C603A molecules may exist in cells in close proximity (**Figure 5**). Given the fact that C603A retained full expression, plasma membrane targeting, and MX efflux activity comparable to wild-type protein (**Figure 1–3**), we would argue that the intermolecular disulfide bond formed by Cys^{603} alone may not be essential for dimerization or oligomerization of BCRP *in vivo*. It is likely that, besides the intermolecular disulfide bond formed via Cys^{603}, there seems to be intermolecular disulfide bonds formed by other cysteine residues or non-covalent interactions that also contribute to dimer/oligomer formation of BCRP. For example, it has been shown that, in addition to Cys^{603}, Cys^{592} and Cys ^{608} may be also potentially involved in intermolecular disulfide bond formation of BCRP [25].

In conclusion, we, for the first time, have provided direct evidence that wild-type BCRP can form dimers or oligomers *in vivo* in intact mammalian cells using the FRET microscopy. We have also shown that the intermolecular disulfide bond formed by Cys^{603} alone may not be essential for dimer/oligomer formation of BCRP *in vivo*. This information provides a basis for further structural and mechanistic analysis of BCRP and related ABC transporters.

Acknowledgements

We thank Dr. Susan E. Bates (National Cancer Institute, Bethesda, MD) for providing the full-length wild-type human BCRP cDNA. We gratefully acknowledge financial support from the National Institutes of Health (GM073715). Michelle E. Mark was a recipient of the Mary Gates Research Scholarship from the University of Washington.

Please address correspondence to: Qingcheng Mao, PhD, Department of Pharmaceutics, School of Pharmacy, Box 357610, University of Washington, Seattle, WA 98195-7610; Tel: (206) 685-0355; Fax: (206) 543-3204; Email: qmao@u.washington.edu

Abbreviations

BCRP, breast cancer resistance protein; ABC, ATP-binding cassette; ABCG2, ATP binding cassette G2; HEK, human embryonic kidney; NBD, nucleotide-binding domain; MSD, membrane-spanning domain; TM, transmembrane; FRET, fluorescence resonance energy transfer; MX, mitoxantrone; FTC, fumitremorgin C; EDTA, ethylenediaminetetraacetic acid; FBS, fetal bovine serum; BSA, bovine serum albumin; mAb, monoclonal antibody; DMSO, dimethyl sulfoxide; MEM, Eagle's minimum essential medium; PBS, phosphate-buffered saline; PCR, polymerase chain reaction; SDS, sodium dodecyl sulfate; CFP, cyan fluorescence protein; YFP, yellow fluorescence protein; DSS, disuccinimidyl suberate.

References

[1] Mao Q, and Unadkat JD. Role of the breast cancer resistance protein (ABCG2) in drug transport. Aaps J 2005; 7:E118-133.
[2] Robey RW, To KK, Polgar O, Dohse M, Fetsch P, Dean M, and Bates SE. ABCG2: a perspective. Adv Drug Deliv Rev 2009; 61:3-13.
[3] Zhang JT. Biochemistry and pharmacology of the human multidrug resistance gene product, ABCG2. Zhong Nan Da Xue Xue Bao Yi Xue Ban 2007; 32:531-541.
[4] Robey RW, Polgar O, Deeken J, To KW, and Bates SE. ABCG2: determining its relevance in clinical drug resistance. Cancer Metastasis Rev 2007; 26:39-57.
[5] Zhou S, Morris JJ, Barnes Y, Lan L, Schuetz JD, and Sorrentino BP. Bcrp1 gene expression is required for normal numbers of side population stem cells in mice, and confers relative protection to mitoxantrone in hematopoietic cells in vivo. Proc Natl Acad Sci U S A 2002; 99:12339-12344.
[6] Zhou S, Schuetz JD, Bunting KD, Colapietro AM, Sampath J, Morris JJ, Lagutina I, Grosveld GC, Osawa M, Nakauchi H, and Sorrentino BP. The ABC transporter Bcrp1/ABCG2 is expressed in a wide variety of stem cells and is a molecular determinant of the side-population phenotype. Nat Med 2001; 7:1028-1034.
[7] Maliepaard M, Scheffer GL, Faneyte IF, van

Gastelen MA, Pijnenborg AC, Schinkel AH, van De Vijver MJ, Scheper RJ, and Schellens JH. Subcellular localization and distribution of the breast cancer resistance protein transporter in normal human tissues. Cancer Res 2001; 61:3458-3464.
[8] Cooray HC, Blackmore CG, Maskell L, and Barrand MA. Localisation of breast cancer resistance protein in microvessel endothelium of human brain. Neuroreport 2002; 13:2059-2063.
[9] Cisternino S, Mercier C, Bourasset F, Roux F, and Scherrmann JM. Expression, up-regulation, and transport activity of the multidrug-resistance protein Abcg2 at the mouse blood-brain barrier. Cancer Res 2004; 64:3296-3301.
[10] Wang H, Wu X, Hudkins K, Mikheev A, Zhang H, Gupta A, Unadkat JD, and Mao Q. Expression of the breast cancer resistance protein (Bcrp1/Abcg2) in tissues from pregnant mice: effects of pregnancy and correlations with nuclear receptors. Am J Physiol Endocrinol Metab 2006; 291:E1295-1304.
[11] Polgar O, Robey RW, and Bates SE. ABCG2: structure, function and role in drug response. Expert Opin Drug Metab Toxicol 2008; 4:1-15.
[12] Sarkadi B, Homolya L, Szakacs G, and Varadi A. Human multidrug resistance ABCB and ABCG transporters: participation in a chemoimmunity defense system. Physiol Rev 2006; 86: 1179-1236.
[13] Doyle L, Yang W, Abruzzo LV, Krogmann T, Gao Y, Rishi AK, and Ross DD. A multidrug resistance transporter from human MCF-7 breast cancer cells. Proc Natl Acad Sci U S A 1998; 95:15665-15670.
[14] Miyake K, Mickley L, Litman T, Zhan Z, Robey R, Cristensen B, Brangi M, Greenberger L, Dean M, Fojo T, and Bates SE. Molecular cloning of cDNAs which are highly overexpressed in mitoxantrone-resistant cells: demonstration of homology to ABC transport genes. Cancer Res 1999; 59:8-13.
[15] Kusuhara H, and Sugiyama Y. ATP-binding cassette, subfamily G (ABCG family). Pflugers Arch 2007; 453:735-744.
[16] Kage K, Tsukahara S, Sugiyama T, Asada S, Ishikawa E, Tsuruo T, and Sugimoto Y. Dominant-negative inhibition of breast cancer resistance protein as drug efflux pump through the inhibition of S-S dependent homodimerization. Int J Cancer 2002; 97:626-630.
[17] Bhatia A, Schafer HJ, and Hrycyna CA. Oligomerization of the human ABC transporter ABCG2: evaluation of the native protein and chimeric dimers. Biochemistry 2005; 44:10893-10904.
[18] Henriksen U, Fog JU, Litman T, and Gether U. Identification of intra- and intermolecular disulfide bridges in the multidrug resistance transporter ABCG2. J Biol Chem 2005; 280:36926-36934.
[19] Xu J, Liu Y, Yang Y, Bates S, and Zhang JT. Characterization of oligomeric human half-ABC transporter ATP-binding cassette G2. J Biol Chem 2004; 279:19781-19789.
[20] McDevitt CA, Collins RF, Conway M, Modok S, Storm J, Kerr ID, Ford RC, and Callaghan R. Purification and 3D structural analysis of oligomeric human multidrug transporter ABCG2. Structure 2006; 14:1623-1632.
[21] Xu J, Peng H, Chen Q, Liu Y, Dong Z, and Zhang JT. Oligomerization domain of the multidrug resistance-associated transporter ABCG2 and its dominant inhibitory activity. Cancer Res 2007; 67:4373-4381.
[22] Wang H, Lee EW, Cai X, Ni Z, Zhou L, and Mao Q. Membrane topology of the human breast cancer resistance protein (BCRP/ABCG2) determined by epitope insertion and immunofluorescence. Biochemistry 2008; 47:13778-13787.
[23] Kage K, Fujita T, and Sugimoto Y. Role of Cys-603 in dimer/oligomer formation of the breast cancer resistance protein BCRP/ABCG2. Cancer Sci 2005; 96:866-872.
[24] Wakabayashi K, Nakagawa H, Adachi T, Kii I, Kobatake E, Kudo A, and Ishikawa T. Identification of cysteine residues critically involved in homodimer formation and protein expression of human ATP-binding cassette transporter ABCG2: a new approach using the flp recombinase system. J Exp Ther Oncol 2006; 5:205-222.
[25] Liu Y, Yang Y, Qi J, Peng H, and Zhang JT. Effect of cysteine mutagenesis on the function and disulfide bond formation of human ABCG2. J Pharmacol Exp Ther 2008; 326:33-40.
[26] Fjorback AW, Pla P, Muller HK, Wiborg O, Saudou F, and Nyengaard JR. Serotonin transporter oligomerization documented in RN46A cells and neurons by sensitized acceptor emission FRET and fluorescence lifetime imaging microscopy. Biochem Biophys Res Commun 2009; 380:724-728.
[27] Qu Q, and Sharom FJ. FRET analysis indicates that the two ATPase active sites of the P-glycoprotein multidrug transporter are closely associated. Biochemistry 2001; 40:1413-1422.
[28] Weinglass AB, Swensen AM, Liu J, Schmalhofer W, Thomas A, Williams B, Ross L, Hashizume K, Kohler M, Kaczorowski GJ, and Garcia ML. A high-capacity membrane potential FRET-based assay for the sodium-coupled glucose co-transporter SGLT1. Assay Drug Dev Technol 2008; 6:255-262.
[29] Hillebrand M, Verrier SE, Ohlenbusch A, Schafer A, Soling HD, Wouters FS, and Gartner J. Live cell FRET microscopy: homo- and heterodimerization of two human peroxisomal ABC transporters, the adrenoleukodystrophy protein (ALDP, ABCD1) and PMP70 (ABCD3). J Biol Chem 2007; 282:26997-27005.
[30] Schmid JA, Scholze P, Kudlacek O, Freissmuth M, Singer EA, and Sitte HH. Oligomerization of the human serotonin transporter and of the rat GABA transporter 1 visualized by fluorescence resonance energy transfer microscopy in living

cells. J Biol Chem 2001; 276:3805-3810.
[31] Orban TI, Seres L, Ozvegy-Laczka C, Elkind NB, Sarkadi B, and Homolya L. Combined localization and real-time functional studies using a GFP -tagged ABCG2 multidrug transporter. Biochem Biophys Res Commun 2008; 367:667-673.
[32] Ozvegy-Laczka C, Laczko R, Hegedus C, Litman T, Varady G, Goda K, Hegedus T, Dokholyan NV, Sorrentino BP, Varadi A, and Sarkadi B. Interaction with the 5D3 monoclonal antibody is regulated by intramolecular rearrangements but not by covalent dimer formation of the human ABCG2 multidrug transporter. J Biol Chem 2008; 283:26059-26070.
[33] Vethanayagam RR, Wang H, Gupta A, Zhang Y, Lewis F, Unadkat JD, and Mao Q. Functional analysis of the human variants of breast cancer resistance protein: I206L, N590Y, and D620N. Drug Metab Dispos 2005; 33:697-705.
[34] Robey RW, Honjo Y, van de Laar A, Miyake K, Regis JT, Litman T, and Bates SE. A functional assay for detection of the mitoxantrone resistance protein, MXR (ABCG2). Biochim Biophys Acta 2001; 1512:171-182.
[35] Gupta A, Zhang Y, Unadkat JD, and Mao Q. HIV protease inhibitors are inhibitors but not substrates of the human breast cancer resistance protein (BCRP/ABCG2). J Pharmacol Exp Ther 2004; 310:334-341.
[36] Ozvegy-Laczka C, Koblos G, Sarkadi B, and Varadi A. Single amino acid (482) variants of the ABCG2 multidrug transporter: major differences in transport capacity and substrate recognition. Biochim Biophys Acta 2005; 1668:53-63.
[37] Rabindran SK, Ross DD, Doyle LA, Yang W, and Greenberger LM. Fumitremorgin C reverses multidrug resistance in cells transfected with the breast cancer resistance protein. Cancer Res 2000; 60:47-50.
[38] Karpova TS, Baumann CT, He L, Wu X, Grammer A, Lipsky P, Hager GL, and McNally JG. Fluorescence resonance energy transfer from cyan to yellow fluorescent protein detected by acceptor photobleaching using confocal microscopy and a single laser. J Microsc 2003; 209:56-70.
[39] Polgar O, Robey RW, Morisaki K, Dean M, Michejda C, Sauna ZE, Ambudkar SV, Tarasova N, and Bates SE. Mutational analysis of ABCG2: role of the GXXXG motif. Biochemistry 2004; 43:9448-9456.
[40] Piston DW, and Kremers GJ. Fluorescent protein FRET: the good, the bad and the ugly, Trends Biochem Sci 2007; 32:407-414.